

Electronic Supplementary Information

Facile preparation of hyaluronic acid and transferrin co-modified Fe₃O₄ nanoparticles with inherent biocompatibility for dual-targeting magnetic resonance imaging of tumors *in vivo*

Jinbin Pan,^{‡^a} Shao-Kai Sun,^{‡^b} Yaqiong Wang,^b Yan-Yan Fu,^b Xuejun Zhang,^b Yi Zhang^c and Chunshui Yu^{*^a}

^a Department of Radiology, Tianjin Key Laboratory of Functional Imaging, Tianjin Medical University General Hospital, Tianjin 300052, China. Email: chunshuiyu@tjmu.edu.cn

^b School of Medical Imaging, Tianjin Medical University, Tianjin 300203, China

^c Department of Medical Chemistry, Tianjin Key Laboratory on Technologies Enabling Development of Clinical Therapeutics and Diagnostics (Theranostics), College of Pharmacy, Tianjin Medical University, Tianjin 300070, China

[‡] These authors contributed equally to this work.

Correspondence to: Chunshui Yu (E-mail: chunshuiyu@tjmu.edu.cn)

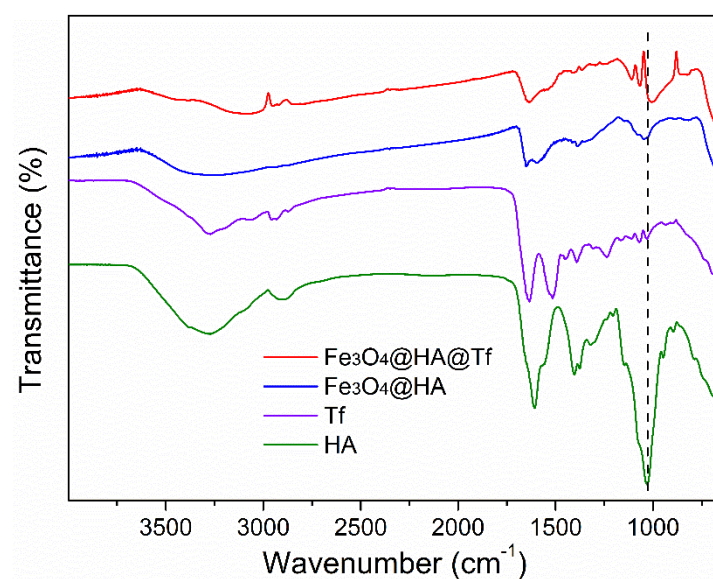


Fig. S1 FT-IR spectra of Fe₃O₄@HA@Tf NPs, Fe₃O₄@HA NPs, Tf and HA.

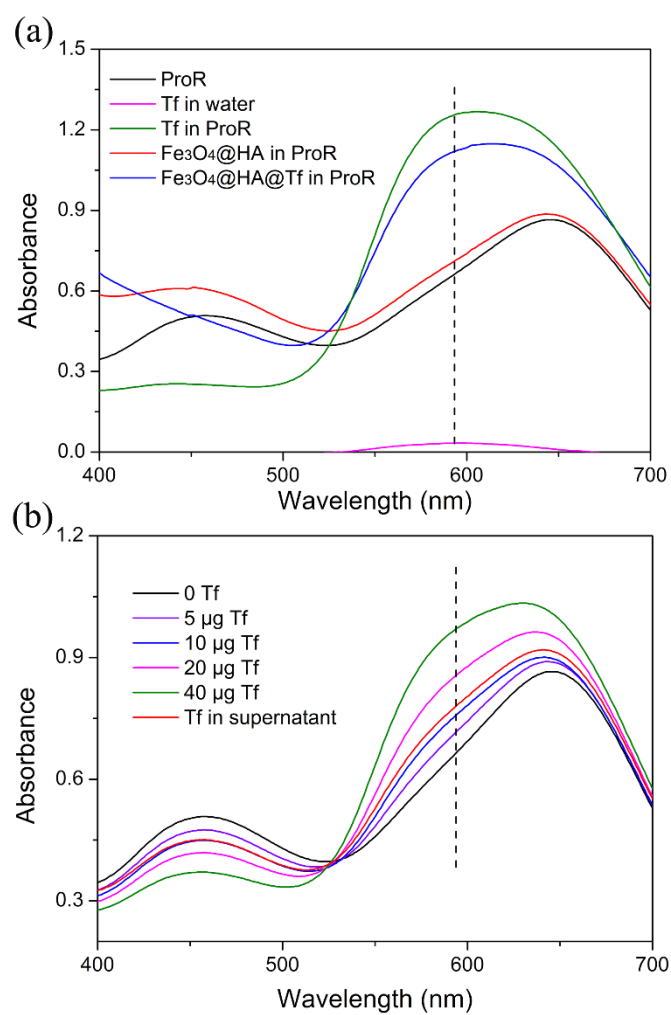


Fig. S2 UV-vis-NIR absorption spectra of different solutions in Bradford

protein assay. (a) ProR, Tf in water, Tf in ProR, $\text{Fe}_3\text{O}_4@\text{HA}@$ NPs in ProR and $\text{Fe}_3\text{O}_4@\text{HA}@\text{Tf}$ NPs in ProR; (b) Various concentrations of Tf in ProR and supernatant containing unreacted Tf in ProR. ProR meant protein reagent was prepared according to Bradford protein assay: 5 mg of coomassie brilliant blue G-250 was dissolved in the mixture of ethanol and phosphoric acid, then the resulted solution was diluted to a final volume of 50 mL for subsequent use. The mixture of ProR and Tf induced a strong absorption at 595 nm due to the special interaction between them. The mixture of ProR and $\text{Fe}_3\text{O}_4@\text{HA}@\text{Tf}$ NPs showed an obviously increasing absorption at 595 nm compared with the spectra of ProR itself. However, the mixture of ProR and $\text{Fe}_3\text{O}_4@\text{HA}$ NPs presented negligible increasing absorption at 595 nm (a). So it could be concluded that the Tf was successfully modified on the surface of $\text{Fe}_3\text{O}_4@\text{HA}$ NPs. To further determine the content of Tf in the $\text{Fe}_3\text{O}_4@\text{HA}@\text{Tf}$ NPs, the concentration of free Tf in the supernatant after the conjugation reaction was calculated according to the standard curve of absorbance at 595 nm of Tf in ProR (b). Then the amount of conjugated Tf was deduced by subtracting the amount of free Tf from the amount of added Tf.

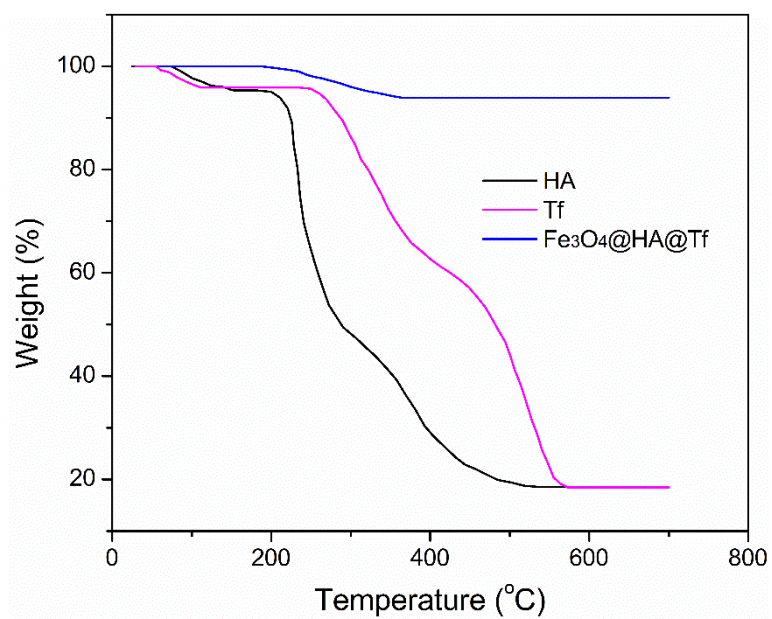


Fig. S3 TGA curves of Fe₃O₄@HA@Tf NPs, HA and Tf, respectively.

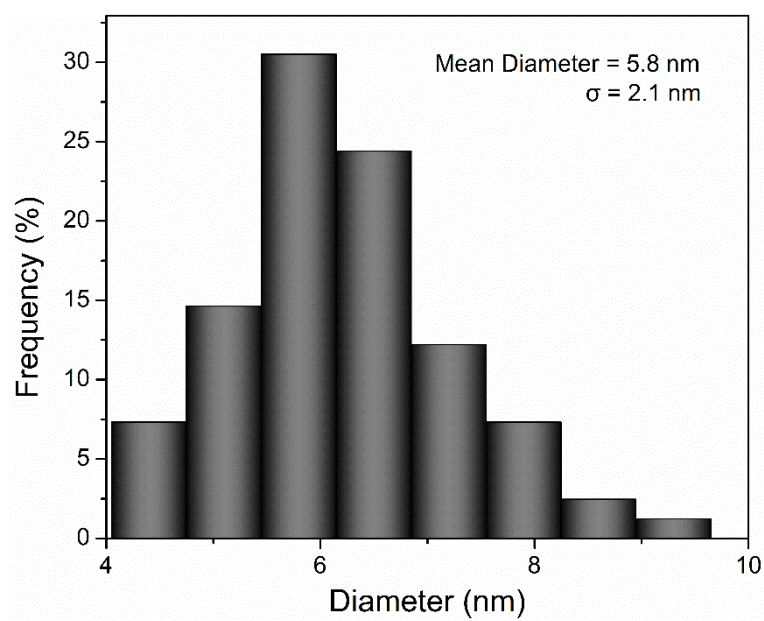


Fig. S4 Size distribution of Fe₃O₄@HA@Tf NPs via the characterization of HRTEM.

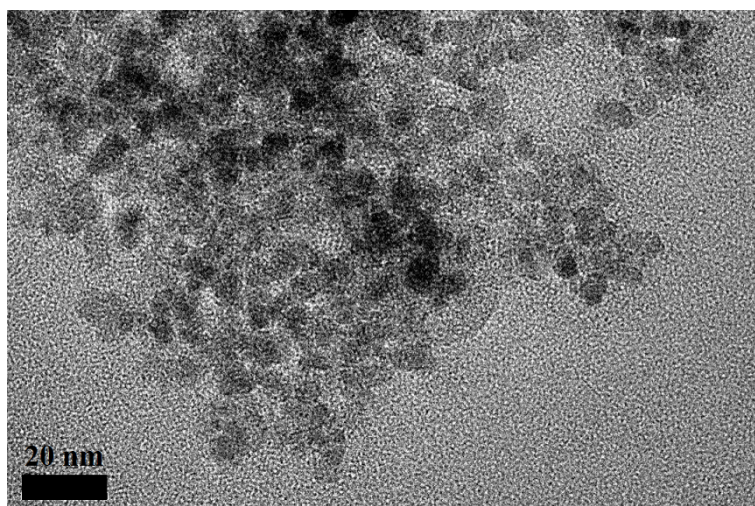


Fig. S5 HRTEM image of $\text{Fe}_3\text{O}_4@\text{HA}$ NPs.

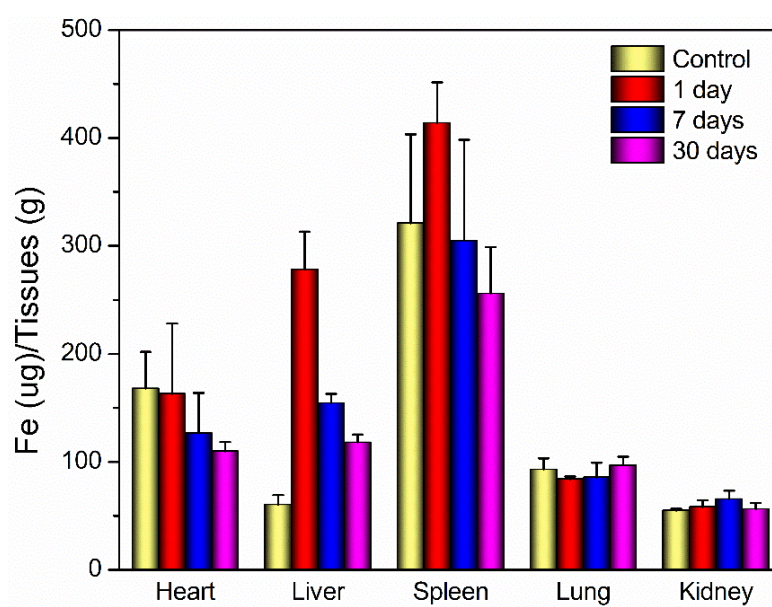


Fig. S6 Distribution of Fe in different organs of mice at different time points (1, 7, 30 days) after intravenous administration of $\text{Fe}_3\text{O}_4@\text{HA}@\text{Tf}$ NPs in PBS (24 mg Fe/kg). Mice without treatments of the nanoprobe were regarded as control group, n=3.

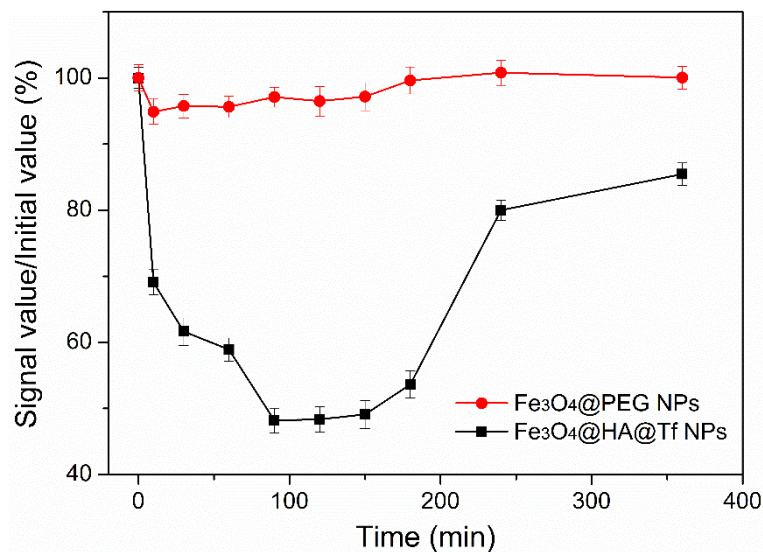


Fig. S7 The changes of MR signal intensity of tumor sites before and after administration of Fe₃O₄@HA@Tf NPs and Fe₃O₄@PEG NPs in PBS (24 mg Fe/kg) at different time points post-injection of the nanoprobes, respectively.

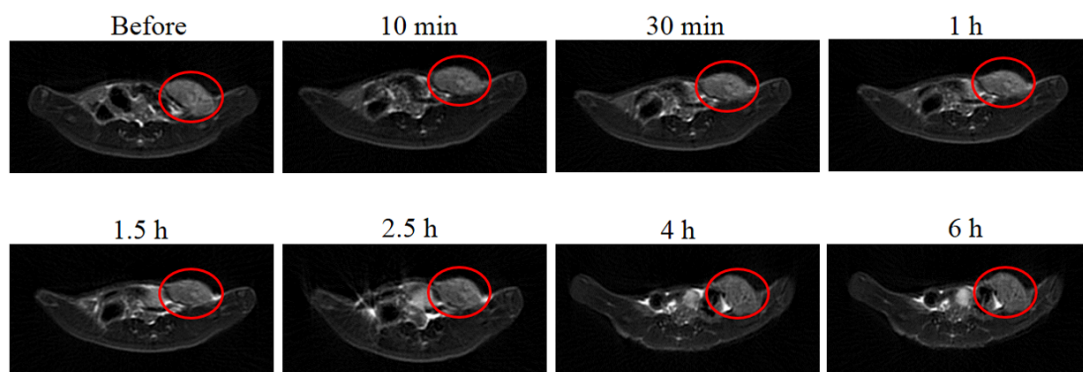


Fig. S8 T₂-weighted MR images of tumor-bearing mouse before and after intravenous administration of Fe₃O₄@PEG NPs in PBS (24 mg Fe/kg) at different time points. The region with red cycle was tumor site.

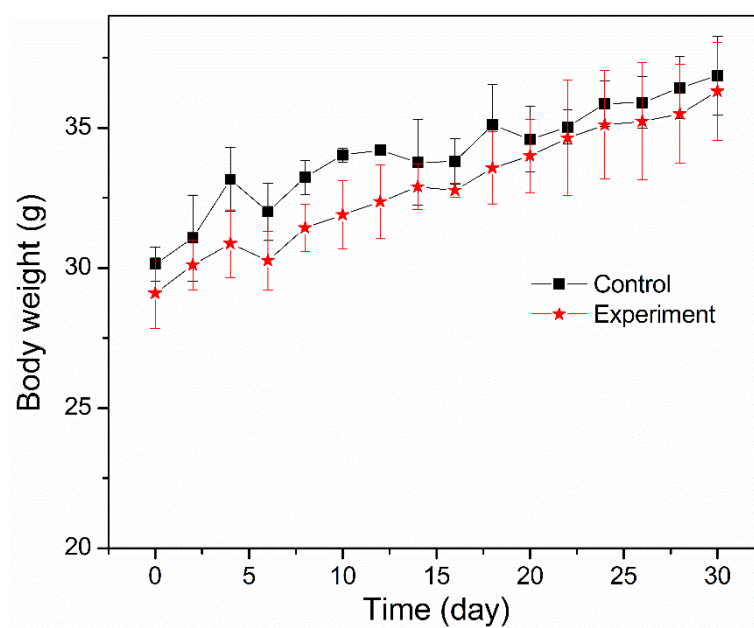


Fig. S9 Body weight of mice after intravenous administration of $\text{Fe}_3\text{O}_4@\text{HA}@\text{Tf}$ NPs in PBS (24 mg Fe/kg), n=3.